Detecting Time Irreversibility Using Quantile Autoregressive Models

Alain Hecq* **Li Sun†**

November 29, 2017

Preliminary version, do not quote[1]

Abstract

The aim of this paper is twofold. First we propose to detect time irreversibility in stationary time series using quantile autoregressive models (QAR). We show that this approach provides an alternative way to identify causal from noncausal models. Although we obviously assume non-Gaussian disturbances, we do not need any parametric likelihood function to be maximized (e.g. the Student or the Cauchy). This is very interesting for skewded distributions for instance. Secondly, we propose to extend QAR models to quantile regressions in reverse time. This new modelling is appealing for investigating the presence of bubbles in economic and financial time series. We illustrate our analysis using hyperinflation episodes in Latin American countries.

JEL Codes: C22

Keywords: nonlinear time series, quantile autoregressions, mixed causal noncausal models, bubbles, hyperinflation, asymmetric cycles, non-Gaussian errors.

1 Motivation

Mixed causal and noncausal time series models have been recently used in order (i) to obtain a stationary solution to explosive autoregressive processes, (ii) to improve forecast accuracy, (iii) to model expectation mechanisms implied by economic theory, (iv) to interpret non-fundamental shocks resulting from the asymmetric information between economic agents and econometricians,

*Corresponding author: Maastricht University, School of Business and Economics, Department of Quantitative Economics, P.O.Box 616, 6200 MD Maastricht, The Netherlands. Email: a.hecq@maastrichtuniversity.nl

†Maastricht University, School of Business and Economics, Department of Quantitative Economics. Email: l.sun@maastrichtuniversity.nl

[1]The authors would like to thank Hanno Reuvers and Sean Telg for helpful comments.

(v) to generate non-linear features from simple linear models with non-Gaussian disturbances, (vi) to test for time reversibility. When the distribution of the error term is known, a non-Gaussian likelihood approach can be used to discriminate between different lag and lead polynomials of the dependent variable. For instance, the $\mathcal{R}$ package `MARX` developed by Hecq, Lieb and Telg (2017) estimates univariate mixed models under the assumption of a Student 's $t-$distribution with v degrees of freedom (see also Lanne and Saikkonen, 2011, 2013) as well as the Cauchy as a special case of the Student's t when $v = 1$. Gouriéroux and Zakoian (2016) privilege the latter distribution in order to derive analytical results. Gouriéroux and Zakoian (2015), Fries and Zakoian (2017) provide some additional flexibility, such as the possibility to have some skewness, using the family of alpha-stable distributions. Still all those aforementioned results require the estimation of a parametric form. In this article we take another route.

Indeed, the contribution of this paper is twofold. First we propose to detect time irreversibility in stationary time series using quantile autoregressive models (QAR hereafter, see Koenker and Xiao, 2006). We use the QAR approach as well as noncausal version of the QAR (QNCAR hereafter) that we introduce in this paper, as an alternative way to identify purely causal from purely noncausal models. Although we obviously also need that non-Gaussian disturbances generate series we do not make any parametric distributional assumption about the errors. A simple inspection of the sum of rescaled absolute residuals for different quantiles helps to detect the presence of time irreversibility. Secondly, as the QAR versus QNCAR strategy works pretty well for detecting causality from noncausality in the single regime case, we also propose a quantile regression framework in reverse time as the mechanism generating the data. This new modelling is appealing for investigating the presence of bubbles in economic and financial time series and can intuitively be seen as a mixture between the noncausal approach of Gouriéroux and Zakoian (2015), Fries and Zakoian (2017) and the local explosive root framework surveyed for instance in Homm and Breitung (2012).

The rest of the paper is as follows. Section 2 summarizes the main results and the notations needed to understand mixed causal and noncausal models. In Section 3 we present the QAR and the QNCAR model in an heuristic manner; we show how they can inform us about the causal or the noncausal direction using the sum of rescaled absolute residuals for different quantiles. Section 4 proposes a new noncausal quantile model as the mechanism generating multiple regimes with noncausal dynamics. We illustrate our analysis on hyperinflation episodes in Latin American countries in Section 5. Section 6 concludes.

2 Causal and noncausal time series models

Brockwell and Davis introduce in their texbooks (1991, 2002) a univariate noncausal specification as a way to rewrite an autoregressive process with explosive roots into a process in reverse time with roots outside the unit circle. This noncausal process possesses a stable forward looking solution whereas the explosive autoregressive process in direct time does not. This approach can

be generalized to allow for both lead and lag polynomials. This is the so called mixed causal-noncausal univariate autoregressive process for y_t that we denote MAR(r,s)

$$\pi(L)\phi(L^{-1})y_t = \varepsilon_t, \tag{1}$$

where $\pi(L) = 1 - \pi_1 L - ... - \pi_r L^r$, $\phi(L^{-1}) = 1 - \phi_1 L^{-1} - ... - \phi_s L^{-s}$. L is the usual backshift operator that creates lags when raised to positive powers and leads when raised to negative powers, i.e., $L^j y_t = y_{t-j}$ and $L^{-j} y_t = y_{t+j}$. The roots of both polynomials are assumed to lie outside the unit circle, that is $\pi(z) = 0$ and $\phi(z) = 0$ for $|z| > 1$ and therefore

$$y_t = \pi(L)^{-1}\phi(L^{-1})^{-1}\varepsilon_t = \sum_{i=-\infty}^{\infty} a_i \varepsilon_{t-i}. \tag{2}$$

has a infinite two sided moving average representation. We also have that $E(|\varepsilon_t|^\delta) < \infty$ for $\delta > 0$ and the Laurent expansion parameters are such that $\sum_{i=-\infty}^{\infty} |a_i|^\delta < \infty$. The representation (2) is sometimes clearer than (1) to motivate the terminology "causal/noncausal". Indeed those terms refer to as the fact that y_t depends on a causal (resp. noncausal) component $\sum_{i=0}^{\infty} a_i \varepsilon_{t-i}$ (resp. noncausal $\sum_{i=-\infty}^{-1} a_i \varepsilon_{t-i}$). With this in mind, it is obvious that a purely lead equation with explosive coefficients will be defined as a causal model.

Note that in (1), the process y_t is a purely causal MAR$(r,0)$, also known as the conventional causal AR(r) process, when $\phi_1 = ... = \phi_s = 0$,

$$\pi(L)y_t = \varepsilon_t,$$

while the process is a purely noncausal MAR$(0,s)$ model

$$\phi(L^{-1})y_t = \varepsilon_t,$$

when $\pi_1 = ... = \pi_r = 0$.

A crucial point of this literature is that error terms ε_t must be *i.i.d.* non-Gaussian to ensure the identifiability of a causal and a noncausal specification (Breidt, Davis, Lii and Rosenblatt, 1991) and hence to possibly detect time irreversibility in y_t. The departure from Gaussianity is not as such an ineptitude as a large part of macroeconomic and financial time series display nonlinear and non-normal features.

We have already talked in Section 1 about the reasons for looking at models with a lead component. Our main motivation lies in the facts that MAR(r,s) models with non-Gaussian disturbances are able to replicate non-linear features (e.g., bubbles, asymmetric cycles) that previously were usually obtained by highly nonlinear models. As an example, we simulate in Figure 1 a MAR(1,1) such

Figure 1: Simulation of a MAR(1,1) model, T=200

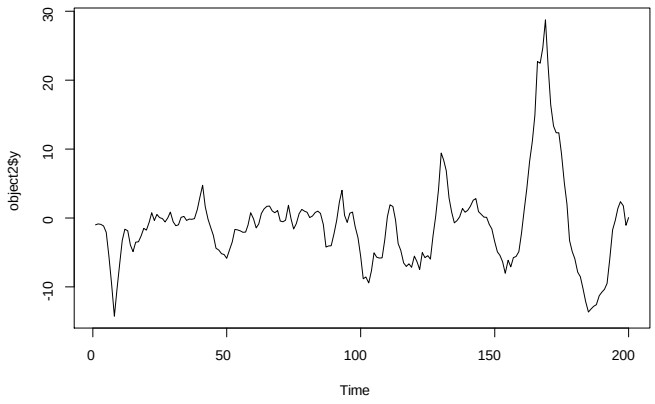

as $(1-0.8L)(1-0.6L^{-1})y_t = \varepsilon_t$ with $\varepsilon_t \tilde{} t(3)$ for 200 observations.[2] One can observe asymmetric cycles and multiple bubbles.

Once a distribution or a group of distributions are chosen, the parameters in $\pi(L)\phi(L^{-1})$ can be estimated by approximate maximum likelihood. Assuming for instance a non-standardized $t-$distribution for the error process the parameters of mixed causal-noncausal autoregressive models of the form (1) can be consistently estimated by approximate maximum likelihood (AML). Let $(\varepsilon_1, ..., \varepsilon_T)$ be a sequence of *i.i.d.* zero mean $t-$distributed random variables, then its joint probability density function can be characterized as

$$f_\varepsilon(\varepsilon_1, ..., \varepsilon_T|\sigma, \nu) = \prod_{t=1}^{T} \frac{\Gamma(\frac{\nu+1}{2})}{\Gamma(\frac{\nu}{2})\sqrt{\pi\nu}\sigma} \left(1 + \frac{1}{\nu}\left(\frac{\varepsilon_t}{\sigma}\right)^2\right)^{-\frac{\nu+1}{2}}.$$

The corresponding (approximate) log-likelihood function, conditional on the observed data $y = (y_1, ..., y_T)$ can be formulated as

$$\begin{aligned} l_y(\boldsymbol{\phi}, \boldsymbol{\varphi}, \boldsymbol{\lambda}, \alpha|y) = (T-p)\left[\ln(\Gamma((\nu+1)/2)) - \ln(\sqrt{\nu\pi}) - \ln(\Gamma(\nu/2)) - \ln(\sigma)\right] \\ - (\nu+1)/2 \sum_{t=r+1}^{T-s} \ln(1 + ((\pi(L)\phi(L^{-1})y_t - \alpha)/\sigma)^2/\nu), \end{aligned} \tag{3}$$

where $p = r+s$ and $\varepsilon_t = \pi(L)\phi(L^{-1})y_t - \alpha$ replaced by a nonlinear function of the parameters when

[2] We use the package MARX develop in $\mathcal{R}$ by Hecq, Lieb and Telg (2017).

expanding the product of polynomials. The distributional parameters are collected in $\boldsymbol{\lambda} = [\sigma, \nu]'$, with σ representing the scale parameter and ν the degrees of freedom. α denotes an intercept that could be introduced in model (1), $\Gamma(\cdot)$ denotes the gamma function. Thus, the AML estimator corresponds to the solution $\hat{\boldsymbol{\theta}}_{ML} = \arg\max_{\boldsymbol{\theta}\in\Theta} l_y(\boldsymbol{\theta}|y)$, with $\boldsymbol{\theta} = [\boldsymbol{\phi}', \boldsymbol{\varphi}', \boldsymbol{\lambda}'']$ and Θ is a permissible parameter space containing the true value of $\boldsymbol{\theta}$, say $\boldsymbol{\theta}_0$, as an interior point. Since an analytical solution of the score function is not directly available, gradient based numerical procedures can be used to find $\hat{\boldsymbol{\theta}}_{ML}$. If $\nu > 2$, and hence $E(|\varepsilon_t|^2) < \infty$, the AML estimator is $\sqrt{T}$-consistent and asymptotically normal. Lanne and Saikonen (2011) also show that a consistent estimator of the limiting covariance matrix is obtained from the standardized Hessian of the log-likelihood. For the estimation of the parameters and the standard errors as well as for the selection of mixed causal-noncausal models we can also follow the procedure proposed in Hecq, Lieb and Telg (2016).

3 Heuristic results on quantiles regressions for MAR(r,s) models

Koenker and Xiao (2006) have introduced a new quantile autoregressive model of order p, denote QAR(p) such that

$$y_t = \theta_0(u_t) + \theta_1(u_t)y_{t-1} + ... + \theta_p(u_t)y_{t-p}, \tag{4}$$

where u_t is a sequence of *i.i.d.* standard uniform random variables. Provided that the right side of (4) is monotone increasing in u_t, it follows that the $\tau-$th conditional quantile function of y_t can be written as

$$Q_{y_t}(\tau|y_{t-1}, ...y_{t-p}) = \theta_0(\tau) + \theta_1(\tau)y_{t-1} + ... + \theta_p(\tau)y_{t-p}. \tag{5}$$

If a realized time series $\{y_t\}_{t=1}^T$ can be written as QAR(p) model (4), its parameters in (5) can be obtained from the minimization problem

$$\hat{\boldsymbol{\theta}}(\tau) = \min_{\boldsymbol{\theta}\in\mathbb{R}^{p+1}} \sum_{t=1}^{T} \rho_\tau(y_t - \boldsymbol{x}_t'\boldsymbol{\theta}), \tag{6}$$

where $\rho_\tau(u) := u(\tau - I(u < 0))$ is called the check function; $\boldsymbol{x}_t' = [1, y_{t-1}, \ldots, y_{t-p}]$; $\boldsymbol{\theta} = [\theta_0, \theta_1, \ldots, \theta_{t-p}]$. We define the sum of rescaled absolute residuals (SRAR hereafter) for each pair of $(\tau, \boldsymbol{\theta})$ as

$$\text{SRAR}(\tau, \boldsymbol{\theta}) := \sum_{t=1}^{T} \rho_\tau(y_t - \boldsymbol{x}_t'\boldsymbol{\theta}). \tag{7}$$

Clearly, the estimated $\hat{\boldsymbol{\theta}}$ for model (5) has the minimum value among $\left\{\text{SRAR}_\tau(\boldsymbol{\theta})|\boldsymbol{\theta} \in \mathbb{R}^{p+1}\right\}$. The simplex algorithm can be used to solve the minimization problem (6) and parameters for each $\tau-$th can easily be estimated in $\mathcal{R}$ using the `qr()` command or in Eviews for instance. We extend

Figure 2: Plot of a one-regime process with $N(0,1)$ errors, $T = 200$

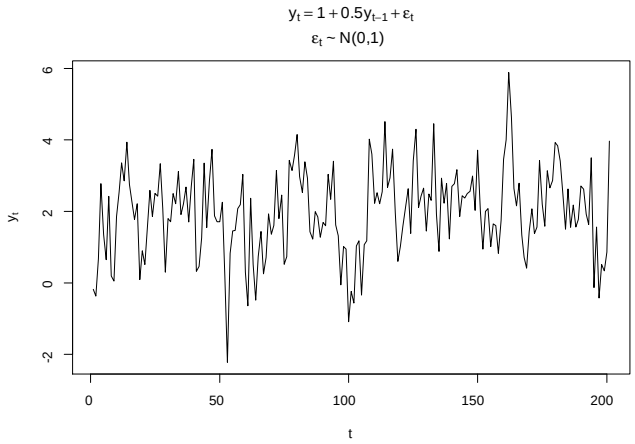

the model (5) to have a noncausal quantile counterpart[3] that we denote QNCAR(p) such as

$$Q_{y_t}(\tau|y_{t+1}, ...y_{t+p}) = \tilde{\theta}_0(\tau) + \tilde{\theta}_1(\tau)y_{t+1} + ... + \tilde{\theta}_1(\tau)y_{t+p}. \tag{8}$$

Parameters in (8) are estimated similarly as for the QAR(p) model in (5). Next subsections assess how (5) and (8) behave for different data generating processes starting from an autoregressive model with Gaussian disturbances to more heavy tails distributions.

3.1 Causal models with Gaussian i.i.d. disturbances

Suppose first that the process $\{y_t\}$ follows for $T = 200$ observation an autoregressive process of order 1, $y_t = \alpha + \beta y_{t-1} + \varepsilon_t$, where $[\alpha, \beta] = [1, 0.5]$ and $\{\varepsilon_t\}$ are *i.i.d.* standard normal distributed for $T = 200$. Fig. 2 displays a simulated series. Applying a quantile regression method using `rq()` on the generated data gives the estimation results reported in Fig. 3 for a QAR specification (5) and in Fig. 4 for a QNCAR specification (8). The straight dashed lines represent OLS estimated parameters. We do not report the confidence intervals around quantile regression coefficients but it is obvious that no pattern emerges, especially for the slope parameters. They stay pretty stable among conditional quantile regressions.

The information displayed in Figure 5 will be used to detect the presence of time irreversibility. It shows the sum of rescaled absolute residuals (SRAR) for different quantiles. The two curves,

[3]Note that mixed causal noncausal models are under investigation but results are not reported at this earlier stage of our research.

Figure 3: Estimation by causal QAR on an AR(1) with $N(0,1)$ errors, $T = 200$

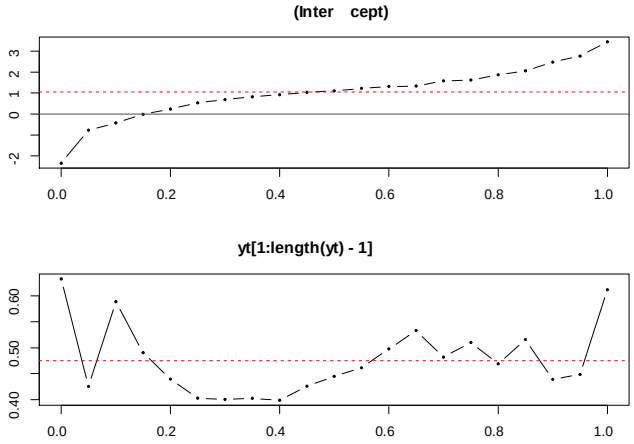

Figure 4: Estimation by noncausal QNCAR of an AR(1) with $N(0,1)$ errors, $T = 200$

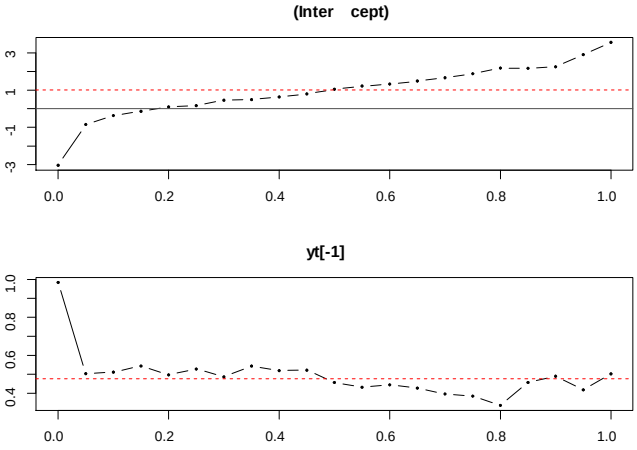

Figure 5: Sum of rescaled absolute residuals along quantiles for an AR(1) with $N(0,1)$ errors, $T = 200$

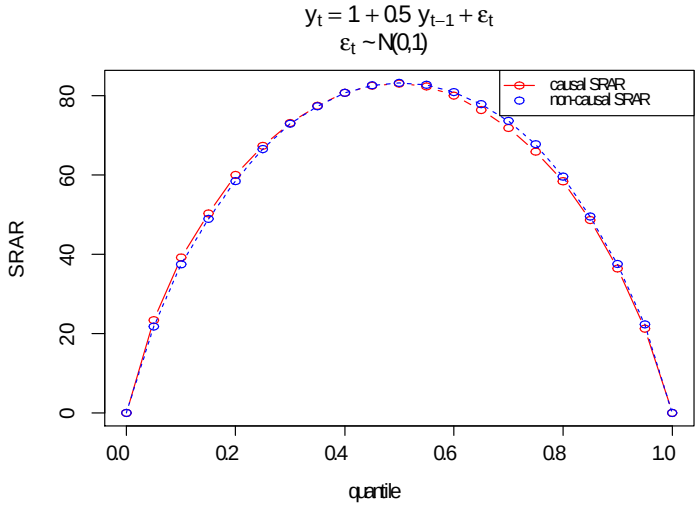

from repetitively QAR and QNCAR estimations, almost overlap at each quantiles. This illustrates that, similarly to OLS, we cannot discriminate between causal and noncausal modes using quantile regressions (5) and (8) with Gaussian disturbances. The Gaussian distribution is indeed time reversible, weak and strict stationary as well. Its first two moments characterize the whole distribution and consequently every quantiles. Note that we obtain similar results from a simulated purely noncausal process $y_t = \alpha + \beta y_{t+1} + \varepsilon_t$, where $[\alpha, \beta] = [1, 0.5]$ and $\{\varepsilon_t\}$ are $i.i.d.$ standard normal distributed. Results are not reported to save space.

3.2 Causal and noncausal models with Student's t distributed errors

Things become different if we depart from Gaussianity. Suppose now an AR(1) process $y_t = \alpha + \beta y_{t-1} + \varepsilon_t$ with again $[\alpha, \beta] = [1, 0.5]$ but where $\{\varepsilon_t\}$ are $i.i.d.$ Student's $t-$distributed with 2 degrees of freedom. Fig. 6 pictures the data for $T = 200$. Applying quantile regressions QAR and QNCAR with `rq()` on this series gives the estimation results as shown in Figures 7 and 8. It is difficult to interpret graphs from a single random draw but we notice that the QAR estimated slope parameter is more stable than the one obtained from QNCAR. The important information is obtained from SRAR curves displayed in Figure 9. The distance between the two curves is much larger than with the Gaussian distribution, favouring for most quantiles the causal causal specification we simulated. Note that the distance increases with the sample size and with the departure from Gaussianity. For instance Figure 10 plots SRAR for series generated by a purely

Figure 6: Plot of an AR(1) with $t(2)$ errors, $T = 200$

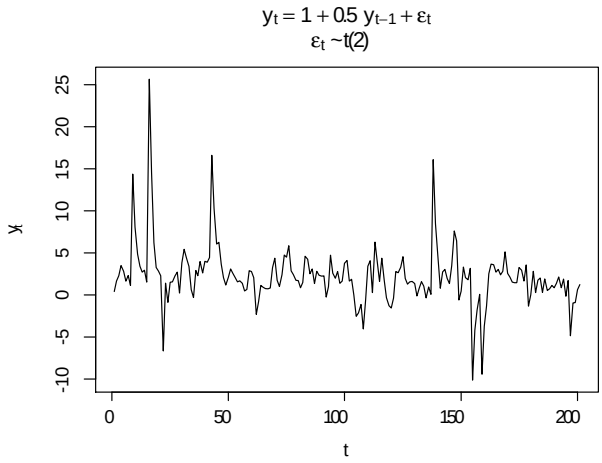

noncausal process with *i.i.d.* Cauchy errors. Figure 11 plots the series. Clearly the noncausal specification has to be preferred. A testing strategy based on the area between those two curves is investigated in the next section.

.

4 Quantile autoregressions as a generating mechanism

So far we have estimated the QAR and its QNCAR extension that we introduce in this paper on purely causal and noncausal model having the same parameters for each quantile. We look now at data generating processes that have potentially different functions for different quantiles. This is the model proposed by Koenker and Xiao (2006).

4.1 Causal QAR

A causal quantile autoregressive time series process of order 1, denoted QAR(1), is now considered as the mechanism generating y_t. As an example we use a three regimes model such that

$$\begin{cases} y_t = \alpha_1 + \beta_1 y_{t-1} & \text{if } 0 \leq \tau_t \leq \tau_1^* \\ y_t = \alpha_2 + \beta_2 y_{t-1} & \text{if } \tau_1^* < \tau_t < \tau_2^* \\ y_t = \alpha_3 + \beta_3 y_{t-1} & \text{if } \tau_2^* \leq \tau_t \leq 1 \end{cases} \tag{9}$$

Figure 7: Estimation by causal quantile regression on an AR(1) with $t(2)$, $T = 200$

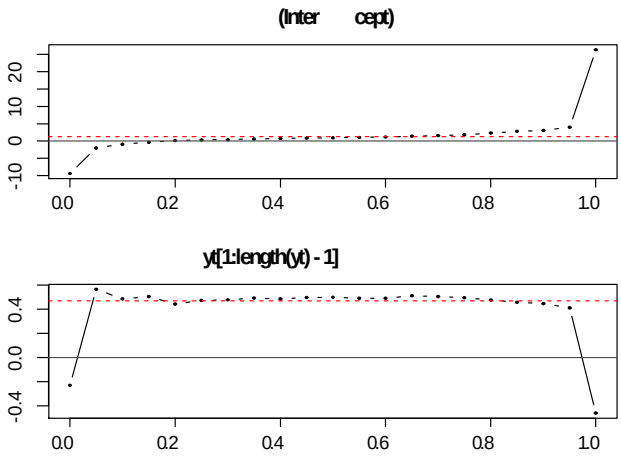

Figure 8: Estimation by non-causal quantile regression on an AR(1) with $t_{(2)}$, $T = 200$

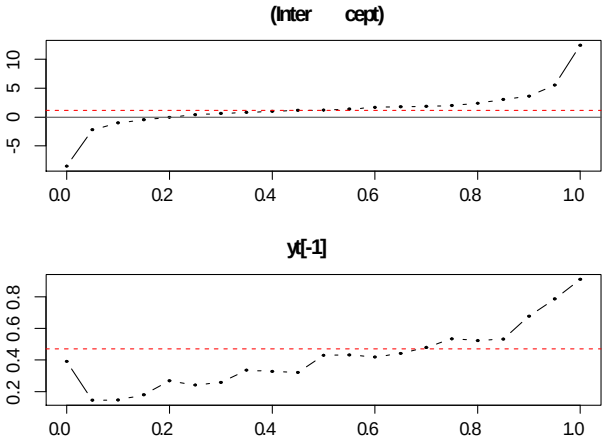

Figure 9: Sum of rescaled absolute residuals along quantiles for an AR(1) with $t_{(2)}$, $T = 200$

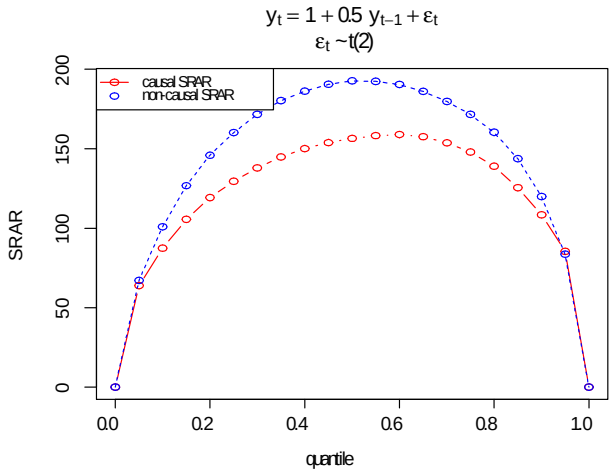

Figure 10: SRAR along quantiles on a noncausal model with Cauchy errors, $T = 200$

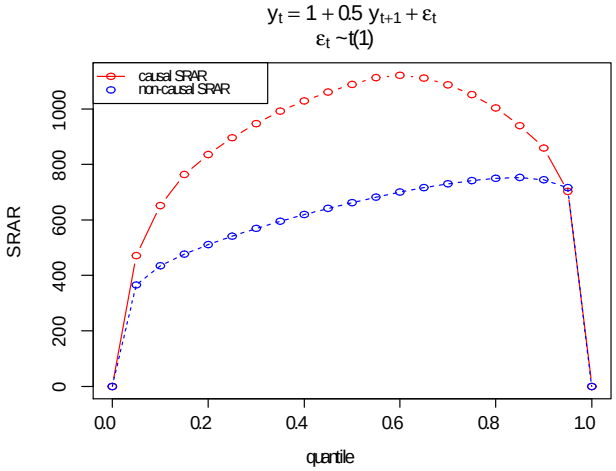

Figure 11: Plot of a noncausal model with Cauchy errors, $T = 200$

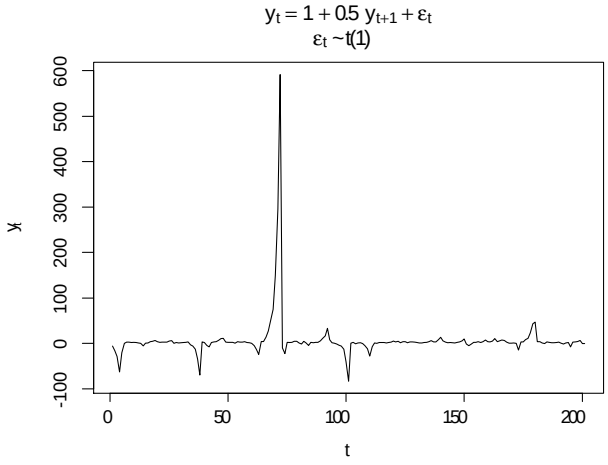

where $\{\tau_t\}$ is a sequence of *i.i.d.* standard uniform random variables, implying that the generated process y_t at t is the quantile $Q_{y_t}(\tau_t|y_{t-1})$. Bubble phenomena can be generated by (9) through assigning different functions to each quantile case. For example, to have a bubble feature in (9), one can simulate (i) a mean-reversion process when $\tau_1^* < \tau_t < \tau_2^*$, (ii) an upward trend with a more persistent root when $\tau_2^* \leq \tau_t \leq 1$, and (iii) when $0 \leq \tau_t \leq \tau_1^*$, a drop is assured to be generated. Note that the coefficient β_3 can also have a unit coefficient or can even be explosive like in the local explosive root literature.

Based on this setting, an intercept vector $\alpha' = [\alpha_1, \alpha_2, \alpha_3]$, a coefficient vector $\beta' = [\beta_1, \beta_2, \beta_3]$ and a threshold quantile vector $\tau^{*\prime} = [\tau_1^*, \tau_2^*]$, for instance, are chosen as follows:

$$\begin{aligned} \alpha' &= [-1.282, 0, 0.842], \\ \beta' &= [0.1, 0.7, 0.9] \\ \tau^{*\prime} &= [0.001, 0.6] \end{aligned} \tag{10}$$

The generated time series with a bubble that bursts around the observation 100 is plotted in Fig. 11 for $T = 200$. The corresponding plot of y_t over y_{t-1} is shown in Fig. 12 where the green colored point is generated in the quantile case $0 \leq \tau_t \leq \tau_1^*$ and the blue colored points are in the case $\tau_2^* \leq \tau_t \leq 1$. This latter graph illustrates the time varying coefficient features of the QAR model.

We now estimate QAR and QNCAR models on the three regimes QAR specification (9) with coefficients (10). The estimation results of a causal quantile regression (5) and the one of a noncausal quantile regression (8) are shown in Fig. 13 and Fig. 14 respectively. We notice that the slope

Figure 12: QAR(1) DGP plot

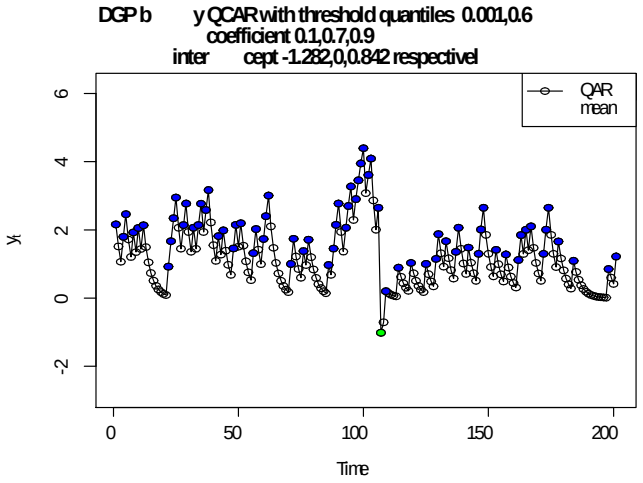

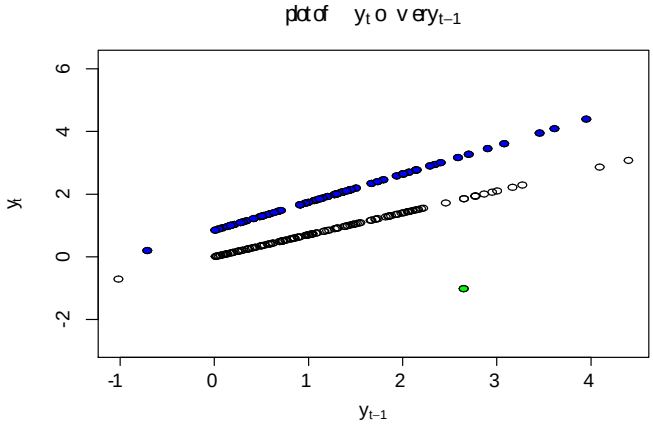

parameters of the QNCAR are possible but unlikely as the coefficient takes large explosive values in one third of the sample. In addition we plot the sum of their respective absolute residuals at each quantile (Fig. 15). It emerges that the QNCAR shows the semi circular pattern observed previously in the single regime case. For the correct causal QAR model we have a different shape with straight lines connecting threshold quantiles. Indeed, the triangular shape of SRAR corresponds to the true model (9). Specifically, suppose $0 < \tau_1 < \tau_2 < \tau_3 < 1$ within the same regime in model (9) of coefficients, say $\alpha(\tau)$ and $\beta(\tau)$ respectively. As SRAR in τ quantile regression is obtained by

$$\begin{aligned} \text{SRAR}(\tau) = \sum_{t=1}^{T} \Big\{ & \tau \left[y_t - (\hat{\alpha}(\tau) + \hat{\beta}(\tau) y_{t-1}) \right]^+ \\ & + (1-\tau) \left[y_t - (\hat{\alpha}(\tau) + \hat{\beta}(\tau) y_{t-1}) \right]^- \Big\}, \end{aligned} \tag{11}$$

where $\hat{\alpha}(\tau), \hat{\beta}(\tau)$ are the estimates; $[\cdot]^+$ denotes the positive part of the inside value and $[\cdot]^-$ denotes the negative part. Any real-valued function f can be written as $f = [f]^+ - [f]^-$. The slope between $\text{SRAR}(\tau_1)$ and $\text{SRAR}(\tau_2)$ is

$$\begin{aligned} \frac{\text{SRAR}(\tau_1) - \text{SRAR}(\tau_2)}{\tau_1 - \tau_2} = \sum_{t=1}^{T} \Big\{ & \left[y_t - (\hat{\alpha}(\tau) + \hat{\beta}(\tau) y_{t-1}) \right]^+ \\ & - \left[y_t - (\hat{\alpha}(\tau) + \hat{\beta}(\tau) y_{t-1}) \right]^- \Big\}, \end{aligned} \tag{12}$$

which is equal to the slope between $\text{SRAR}(\tau_2)$ and $\text{SRAR}(\tau_3)$. Therefore, if the correct model contains few regimes, straight lines connecting threshold quantiles are anticipated in the SRAR plot along quantile, as we see in Figure 15.

4.2 Non-causal QAR - QNCAR

Similarly, a non-causal quantile autoregressive time series y_t is defined as

$$\begin{cases} y_t = \alpha_1 + \beta_1 y_{t+1} & \text{if } 0 \le \tau_t \le \tau_1^* \\ y_t = \alpha_2 + \beta_2 y_{t+1} & \text{if } \tau_1^* < \tau_t < \tau_2^* \\ y_t = \alpha_3 + \beta_3 y_{t+1} & \text{if } \tau_2^* \le \tau_t \le 1 \end{cases}. \tag{13}$$

In order to produce bubble phenomenon we set parameters such that

$$\begin{aligned} \alpha' &= [-0.253, 0, 1.645], \\ \beta' &= [0.8, 0.7, 0.1] \\ \tau^{*\prime} &= [0.4, 0.99] \end{aligned} \tag{14}$$

Figure 13: Estimation by causal quantile regression on the QAR(1) DGP

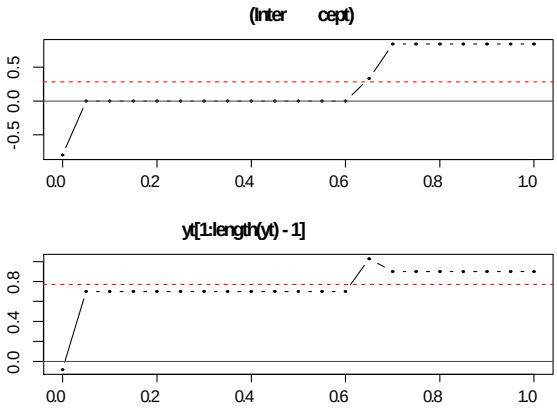

Figure 14: Estimation by non-causal quantile regression on the QAR(1) DGP

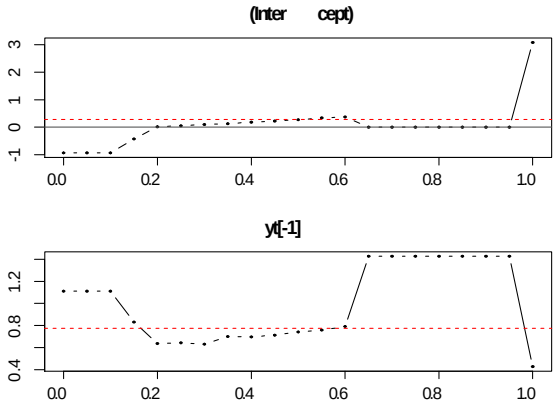

Figure 15: SRAR plot of quantile QAR and QNCAR regressions on the QAR(1) DGP

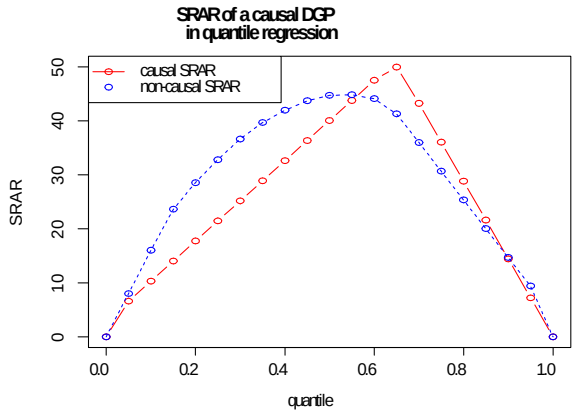

An illustrative plot of a generated non-causal time series is given in Figure 16. Figure 17 and 18 respectively show estimations by QAR and QNCAR. In addition to these two estimations, the SRAR plot is presented in Figure 19.

4.3 Estimation by MARX method

In the introduction we emphasized that the maximum likelihood estimation implemented to detect the presence of time irreverrsibility depends heavily of the distribution chosen. In particular most papers rely on a symmetric distribution with heavy tails such as the Student's t or the Cauchy. We have modified the coefficient β_2 of the second causal regime of the QAR DGP (the other parameters unchanged) to introduce some skewness in the series. Then we estimate models using the Student's t likelihood implemented in the `MARX` package. We fix the lag length of the pseudo causal model at $p = 1$, and we compute the frequencies with which causal and noncausal models are obtained based on 1000 replications. We do not expect very high rates has the `MARX` assumes homogeneity of the parameters. However we observe in Table 1 that when β_2 decreases, the distribution for y_t becomes heavily skewed to the right and the frequency with which we detect an autoregressive model is very low. Instead, when we modify the intercept α_3 in Table 2 with the other parameters unchanged, we do not change the symmetry properties of the generated process. In this case the frequency with which `MARX` predicts an autoregressive model is reasonably high (given the heterogeneity of the AR parameters). QAR and QNCAR estimations are robust to those modifications and we would not switch from a causal to a noncausal identification after the introduction of an asymmetric characteristic.

Figure 16: QNCAR(1) DGP plot

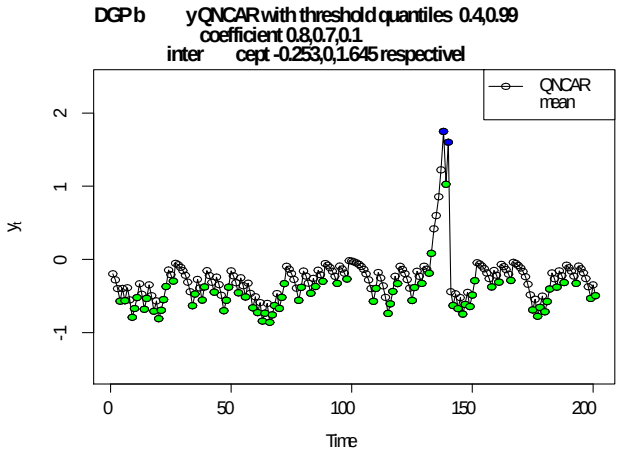

Figure 17: Estimation by QAR on the QNCAR(1) DGP

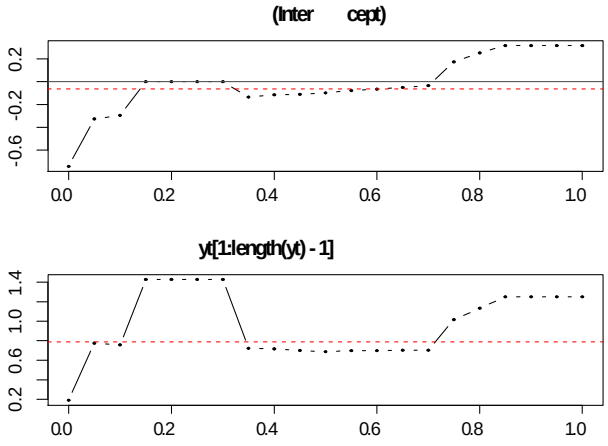

Figure 18: Estimation by QNCAR on the QNCAR(1) DGP

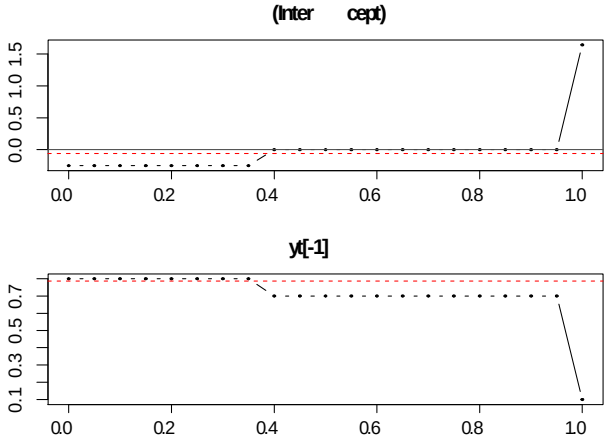

Figure 19: SRAR plot of quantile regression on the QNCAR(1) DGP

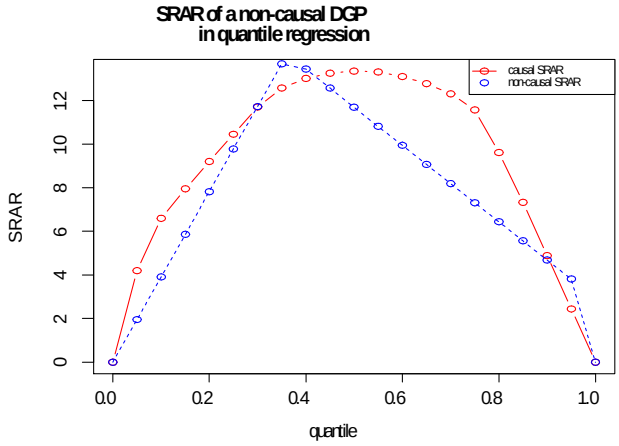

Table 1: Prediction rate of the MAR(1,0) by MARX method over varying β_2 for causal QAR

β_2	correct prediction rate of marx()	unchanged parameters	
0.7	0.853	$\beta_1 = 0.1$	$\alpha_1 = -1.282$
0.6	0.616		$\alpha_2 = 0$
0.5	0.173	$\beta_3 = 0.9$	$\alpha_3 = 0.842$

Table 2: Prediction rate of MARX method over varying α_3 for causal QAR

α_3	correct prediction rate of marx()	unchanged parameters	
1.645	0.853	$\beta_1 = 0.1$	$\alpha_1 = -1.282$
1.282	0.870	$\beta_2 = 0.7$	$\alpha_2 = 0$
0.842	0.864	$\beta_3 = 0.9$	
0.524	0.862		
0.253	0.888		

4.4 SRAR criterion

Given the same number of explanatory variables in quantile regressions, the best model should exhibit the lowest SRAR values. This is similar to the R-squared criterion in the least square regression model. This leads us to use a SRAR criterion whose performance in model selection is going to be evaluated. Table 3 shows both the rates of correct model selection based on the comparison of individual quantile's SRARs of all candidate models and the aggregate SRARs. The aggregate SRAR can be interpreted as an overall performance of a candidate model over quantiles. There are many ways in aggregating SRARs in quantile regression. Two of them are proposed here.

The main issue is to evaluate

$$\int_0^1 SRAR(\tau)d\tau,$$

We approximate the integral by the trapezoidal areas rule. Another method consists in summing all individual SRARs using equal weights. In other words, this aggregation sums all the scores (SRAR(τ), $\tau \in [0,1]$) equally for a candidate model as a measure of its overall performance.

In Table 3, we simulate several processes $\{y_t\}_{t=1}^T$ of size $T = 200$ that we have investigated in Sections 2 and 3. Second, we run quantile regressions in both normal and reverse time. Then we compare their SRARs such as the model with a lower SRAR in each case is selected. This process is repeated 2000 times, and the frequency with which correct models is selected is reported. We observe that if the distribution is Gaussian, none of the model performs best as the frequency with which we find the correct model is about 50%. Now, when $t-$distributed or Cauchy errors are considered we always capture the correct causality direction. The last two columns of Table 3 shows that QAR and QNCAR DGPs are correctly selected. This approach to compare causality directions is used is in the next section.

Table 3: Frequencies of selecting the correct models using the SRAR criterion

Quantiles	model in Fig. 2	model in Fig. 6	model in Fig. 11	model (9)	model (13)
0	0.698	0.678	0.601	0.948	0.931
0.05	0.516	0.416	0.653	0.971	0.928
0.10	0.51	0.677	0.763	0.998	0.928
0.15	0.519	0.858	0.841	0.999	0.925
0.20	0.512	0.948	0.907	1	0.915
0.25	0.513	0.981	0.947	1	0.869
0.30	0.488	0.992	0.978	1	0.82
0.35	0.487	0.998	0.996	1	0.665
0.40	0.486	0.999	0.996	0.987	0.575
0.45	0.487	1	0.996	0.901	0.707
0.50	0.5	1	0.995	0.554	0.912
0.55	0.499	0.999	0.995	0.123	0.987
0.60	0.492	0.999	0.995	0.005	1
0.65	0.478	0.997	0.995	0.12	1
0.70	0.467	0.994	0.979	0.341	0.998
0.75	0.49	0.984	0.951	0.357	0.982
0.80	0.493	0.954	0.903	0.371	0.872
0.85	0.481	0.862	0.858	0.388	0.632
0.90	0.469	0.72	0.791	0.408	0.37
0.95	0.484	0.454	0.668	0.439	0.121
1	0.653	0.58	0.595	0.887	0.871
aggregate SRAR	0.483	0.998	0.995	1	1

5 Modelling hyperinflation in Latin America

A New Keynesian Phillips Curve (NKPC) regression such as

$$\pi_t = \gamma_f \mathbb{E}_t(\pi_{t+1}) + \gamma_b \pi_{t-1} + \beta x_t + \epsilon_t, \tag{15}$$

where π_t denotes inflation, $\mathbb{E}_t(\cdot)$ the conditional expectation at time t is often used to motivate the presence of a noncausal component in inflation series (see Lanne and Luoto, 2013); x_t is a measure for marginal costs and ϵ_t an *i.i.d.* error term. Adding and subtracting $\gamma_f \pi_{t+1}$ and rearranging terms, gives

$$\pi_t = \gamma_f \pi_{t+1} + \gamma_b \pi_{t-1} + \underbrace{\beta x_t + \gamma_f \left(\mathbb{E}_t(\pi_{t+1}) - \pi_{t+1}\right) + \epsilon_t}_{\equiv \eta_{t+1}}, \tag{16}$$

where the newly defined disturbance term η_{t+1} consists of three different parts: (i) the expectation error $(\mathbb{E}_t(\pi_{t+1}) - \pi_{t+1})$ which is assumed *i.i.d.* following the literature on rational expectations models, (ii) the marginal costs variable x_t and (iii) an *iid* error ϵ_t. Subsequently, the newly obtained equation is divided by γ_f and lagged by one period to obtain $(1 - \gamma_f^{-1} L + \gamma_f^{-1} \gamma_b L^2)\pi_t =$

$-\gamma_f^{-1}\eta_t$. In a next step, Lanne and Luoto (2013) show that $a(z) \equiv (1 - \gamma_f^{-1}z + \gamma_f^{-1}\gamma_b z^2)$ can be written as the product of two polynomials, i.e., $a(z) = (1-\phi z)(1-\varphi^* z)$ with $|\phi| < 1$ and $|\varphi^*| > 1$ for plausible values of γ_f and γ leading to a stable mixed causal noncausal formulation.

In this application, we consider seasonally unadjusted quarterly Consumer Price Index (CPI) series for five Latin American countries: Brazil, Mexico, Costa Rica, Chile and Colombia. Raw data are available at the OECD database both at the monthly and the quarterly frequency. Despite the fact that quarterly data are directly available at OECD, we do not consider those series as they are computed from the unweighted average over the three months in the corresponding quarter. Hence, these data are constructed using a linear filter, leading to undesirable properties for the detection of mixed causal and noncausal models (see Hecq, Telg and Lieb, 2017). As a consequence, we use quarterly data using point-in-time sampling.[4]

The first available observation is 1969Q1 for Mexico, 1970Q1 for Chile and Colombia, 1976Q1 for Costa Rica and 1980Q1 for Brazil. The last observation is 2017Q2. We can have some doubts even on quarterly series about the behavior of seasonal unit root tests (here HEGY tests) for such explosive series. Applying seasonal unit roots mechanically, we reject the null of seasonal unit roots in each series whereas we do not reject the null of a unit root at the zero frequency for every series but Chile. This is a bit difficult to believe given the level of the Chilean series. Consequently we compute quarterly inflation rates for the five countries and carry out a regression on seasonal dummies to capture the potential presence of deterministic seasonality. Only for Colombia was the null rejected. Consequently, we substract for that country only the quarterly deterministic components. Figure 19 displays quarterly inflation rates and illustrates the huge inflation episodes that countries have faced.

Table 4 reports for each quarterly inflation rates the autoregressive model obtained using the HQ information criterion as well as the $p - values$ of the Breush-Pagan LM test for the null of no-autocorrelation after having included that number of lags. This shows, with the exception of Costa Rica at a 5% level, that we do not reject the null of no-autocorrelation. Adding lags does not really help to get rid of serial dependence for Costa Rica, thus we keep $p = 4$ lags. Note that we would have obtained more parsimonious models using BIC. However most equation would have suffered from the presence of serial correlation. Next two columns show that for every series we reject the null of no ARCH as well as the null of normality (Jarque-Bera test). We should consequently be able to identify causal from noncausal models. It is not so informative to report values of the coefficients from QAR and QNCAR given the large number of parameters involved. We report instead in Figure 20 the SRAR curves for the five economies. The best model using our SRAR criterion over the whole range of quantiles in reported in the last column of Table 4. We conclude that two countries are purely causal and three countries purely noncausal.

[4] We do not use monthly data in this illustration because monthly inflation series required a very large number of lags. Moreover, the detection of seasonal unit roots in the level of price series was quite difficult. We consequently leave the investigation of monthly price series for further investigations.

Figure 20: Latin America quarterly inflation rates

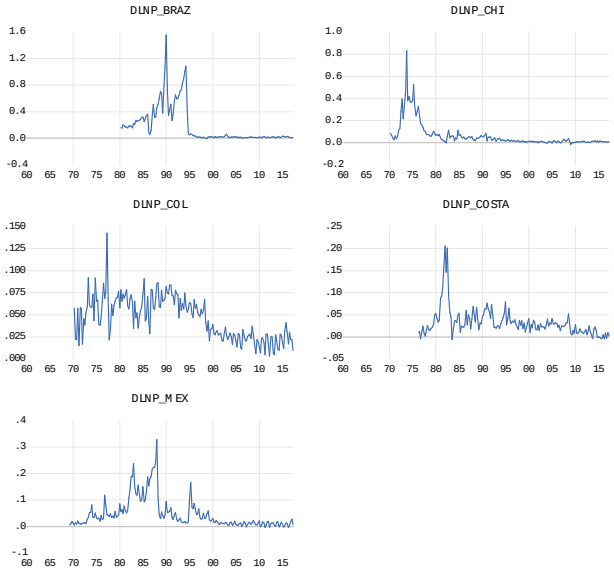

Table 4 - Statistics for inflation rates

Country	HQ	LM[1-2]	BJ	ARCH[1-2]	SRAR
$\Delta \ln P_t^{Bra}$	5	0.27	<0.0001	<0.0001	MAR(0,5)
$\Delta \ln P_t^{Chi}$	8	0.87	<0.0001	<0.0001	MAR(8,0)
$\Delta \ln P_t^{Col}$	12	0.36	<0.0001	0.013	MAR(12,0)
$\Delta \ln P_t^{Costa}$	4	0.04	<0.0001	<0.0001	MAR(0,4)
$\Delta \ln P_t^{Mex}$	10	0.07	<0.0001	<0.0001	MAR(0,10)

Q(N)CAR

SRAR

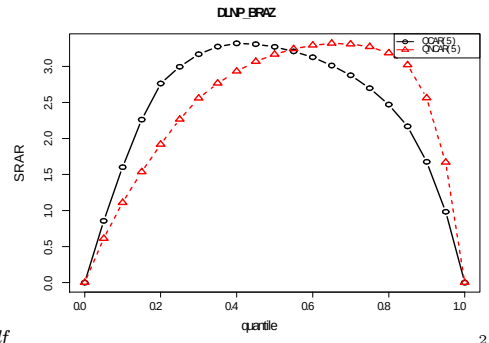

$_{2}2.pdf$

SRAR plot for Brazil

Q(N)CAR

SRAR

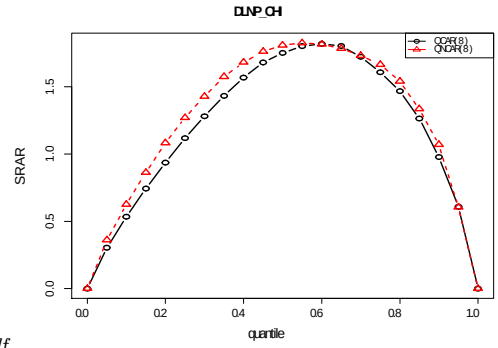

$_{2}3.pdf$

SRAR plot for Chile

Q(N)CAR

SRAR

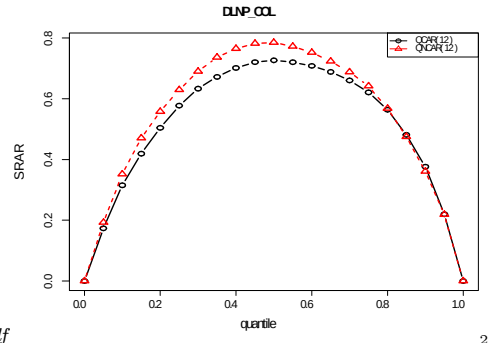

$_{2}4.pdf$

SRAR plot for Colombia

Q(N)CAR

SRAR

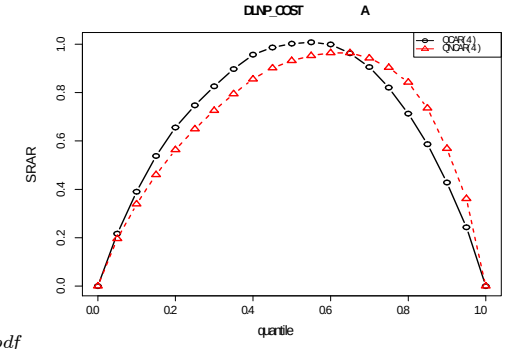

$_{2}5.pdf$

SRAR plot for Costa Rica

Q(N)CAR

SRAR

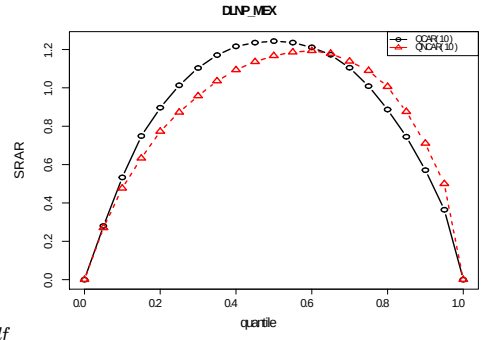

$_{2}6.pdf$

SRAR plot for Mexico

6 Conclusion

This paper introduces a new way to detect causal from noncausal models by comparing estimations from quantile autoregressions developed by Koenker and Xiao (2006) as well as from a similar specification in reverse time. Both models having the same number of parameters we use the sum of rescaled absolute residuals as a criterion to detect models. For inflation rates on five Latin American countries we find that the purely noncausal model is favored in three cases. The mixed model is currently under investigation.

References

[1] Alessi, L., Barigozzi, M. and M. Capasso (2011), Non-Fundamentalness in Structural Econometric Models: A Review. *International Statistical Review 79(1).*

[2] Andrews, B., Davis, R. and F. Breidt (2006), Maximum Likelihood Estimation For All-Pass Time Series Models. *Journal of Multivariate Analysis, 97, 1638-1659.*

[3] Breidt, F., Davis, R., Lii, K. and M. Rosenblatt (1991), Maximum Likelihood Estimation for Noncausal Autoregressive Processes. *Journal of Multivariate Analysis, 36, 175-198.*

[4] Brockwell, P. and R. Davis (1991), *Time Series: Theory and Methods*, Springer-Verlag New York, Second Edition.

[5] Brockwell, P. and R. Davis (2002), *Introduction to Time Series and Forecasting*, Springer-Verlag New York, Second Edition.

[6] Francq, C. and J.-M. Zakoian (2007), HAC Estimation and Strong Linearity Testing in Weak ARMA Models, *Journal of Multivariate Analysis* 98, 114-144.

[7] Fries, S. and J.M. Zakoian (2017), Mixed Causal-Noncausal AR Processes and the Modelling of Explosive Bubbles, Crest discussion paper.

[8] Gouriéroux, C. and J. Jasiak (2017), Misspecification of Causal and Noncausal Orders in Autoregressive Processes, *Journal of Econometrics.*

[9] Gouriéroux, C. and J. Jasiak (2016), Filtering, Prediction and Simulation Methods in Noncausal Processes, *Journal of Time Series Analysis*, doi: 10111/jtsa.12165.

[10] Gouriéroux, C. and J. Jasiak (2015b), Semi-Parametric Estimation of Noncausal Vector Autoregression, *CREST Working Paper, 2015-02.*

[11] Gouriéroux, C. and J.M. Zakoïan (2015), On Uniqueness of Moving Average Representations of Heavy-Tailed Stationary Processes, *Journal of Time Series Analysis*, 36, 876-887.

[12] Gouriéroux, C., and J.M. Zakoïan (2017), Local Explosion Modelling by Noncausal Process, *Journal of the Royal Statistical Society, Series B*, doi:10.1111/rssb.12193.

[13] Hecq, A., Lieb, L. and S. Telg (2016), Identification of Mixed Causal-Noncausal Models in Finite Samples, *Annals of Economics and Statistics*, 123-124.

[14] Hecq, A., Lieb, L., & Telg, S. (2017), Simulation, Estimation and Selection of Mixed Causal-Noncausal Autoregressive Models: The MARX Package. (Social Science Research Network, SSRN).

[15] Hecq, A., Telg, S. and L. Lieb (2017), Do Seasonal Adjustments Induce Noncausal Dynamics in Inflation Rates?, *Econometrics.*

[16] Hencic, A. and C. Gouriéroux (2014), Noncausal Autoregressive Model in Application to Bitcoin/USD Exchange Rate, *Econometrics of Risk, Series: Studies in Computational Intelligence,* Springer International Publishing, 17-40.

[17] Homm, U. and J. Breitung (2012), Testing for Speculative Bubbles in Stock Markets: A Comparison of Alternative Methods, *Journal of Financial Econometrics*, vol.10, 198-231.

[18] Koenker R. and Z. Xiao (2006), Quantile Autoregression, *Journal of the American Statistical Association*, vol. 101, 980-990.

[19] Lanne, M., Luoto J. and P. Saikkonen (2012), Optimal Forecasting of Noncausal Autoregressive Time Series, *International Journal of Forecasting*, 28, 623-631.

[20] Lanne, M. and P. Saikkonen (2011a), Noncausal Autoregressions for Economic Time Series, *Journal of Time Series Econometrics*, 3(3), 1-32.

[21] Lanne, M. and P. Saikkonen (2011b), GMM Estimation with Noncausal Instruments, *Oxford Bulletin of Economics and Statistics*, 73(5), 581-592.

[22] Lanne, M. and P. Saikkonen (2013), Noncausal Vector Autoregression, *Econometric Theory*, 29(3), 447-481.

[23] Lii, K. and Rosenblatt, M. (1993). Non-Gaussian Autoregressive Moving Average Processes. *Proceedings of the National Academy of Science of the United States of America, 90(19), 9168-9170.*

[24] Lippi, M. and L. Reichlin (1993), VAR analysis, nonfundamental representations, Blaschke matrices, *Journal of Econometrics, 63, 307-325.*